

Detection of Bone Cancer Using Region Growing Algorithm and Mean Pixel Intensity Thresholding

¹Madhuri Avula, ¹L. V. Narasimha Prasad and ²Murali Prasad Raja

¹Institute of Aeronautical Engineering, Hyderabad, India

²Vardhaman College of Engineering, Hyderabad, India

Abstract: Cancer, a condition involving unregulated cell growth is a dangerous disease. After many research studies, almost 100 different types of cancers that occur in the human body have been detected. Of these, one of the most common is bone cancer which leads to death. The detection of bone cancer is very arduous and its occurrence is unpredictable. Currently, most studies on cancer exploit data mining methods and the image processing techniques used for medical image analysis. The data and knowledge collected from large databases and related web sites have been used by many scientific researchers for formulating predictions. Association rule mining Supports Vector Machines (SVMs), fuzzy theory and probabilistic neural networks, learning vector quantization, k-means and C-means are the methods most frequently used for the detection, classification and segmentation of bone cancer. In this study, a region growing algorithm has been applied for bone image segmentation. The segmented image is further processed to provide bone cancer detection by evaluating the mean pixel intensity of identified area. Threshold values are proposed for the classification of medical images according to the presence or the absence of bone cancer. This method utilizes jpeg images but can also be applied to medical images in the original format of DICOM (Digital Imaging Communication of Medicine) after some modification. The method provides an accuracy rate of 100% and the required computation time is relatively short.

Key words: Cancer, disease, values, classification, accuracy, analysis

INTRODUCTION

Cancer which involves unregulated cell growth, causes cells to subdivide and increase inexorably, forming malignant tumors that invade nearby parts of the body. The tumors can grow and impede the digestive, nervous and circulatory systems and liberate hormones that alter body functions. Cells become cancer cells because of the damage to DNA. In a normal cell when the DNA is damaged, the cell repairs the damage or the cell dies. If the damaged DNA is not repaired and the cell does not die the damaged DNA causes unnecessary new cells to be formed. Cancer can then enter the bloodstream or lymph nodes. Thus, cancer cells frequently migrate to other parts of the body and begin to produce tumors that replace normal tissues. This process is called metastasis. Many different types of cancers that occur in the human body have been detected. When a malignant tumor directly affects the bone, the disease is known as bone cancer. Bone cancers are called sarcomas. Sarcomas are initiated in muscle, bone, fibrous tissue, blood vessels, fat tissue as well as some other tissues. These cancers can be either primary or secondary. Primary bone cancer is initiated in the bone whereas secondary bone cancer can spread to any location in the body.

The cancer cells located in the bone can even cause bone deformation. Normal bone is constantly being repaired or destroyed and rebuilt. Cancer cells disturb the balance of bone cell growth and formation. If cancer cells are present in the bone the structure of the bone is deformed at a higher rate than that of normal bone.

The pain initially is quite dull but becomes more acute in particular, over the affected part of the bone. The progression related to Ewing sarcoma tends to be faster than that related to other bone cancers. Swelling occurs over the affected part of the bone, a lump forms in the area affected by cancer and the bone begins to degenerate. Moving the joint becomes difficult if the cancer is near a joint. Stress symptoms occur if the tumor grows out from the bone and compresses nearby structures. General symptoms include tiredness, weight loss, sweats, fever and chills as the cancer becomes more advanced. If the cancer spreads to other parts of the body the symptoms may become more severe.

Accurate measurement of alkaline phosphates plays a vital role in the detection of an increase in bone growth activity which is a component of the bone enlargement process. Patients with bone cancer is referred to an oncologist who recommends the following tests. Bone scan: A liquid containing a radioactive substance is

injected into a vein. This substance collects in typical areas and will be detected by the scanner. The image is recorded on a big screen. Computerized Tomography (CT) scan. This scan provides cross sectional images of bones and internal tissues. Using digital geometry, the images can be enlarged and in some cases combined to produce a 3-dimensional image. The results of a CT scan can be used to predict whether or not bone cancer will spread to other parts. Magnetic Resonance Imaging (MRI): MRI uses a magnetic field and radio waves to create comprehensive images of the body an explicit bone or part of a bone. Positron Emission Tomography (PET) scan: PET produces images of the emission a nuclear tracer which is introduced into the body on a biologically active molecules, to produce 3D color images of the processes occurring within the human body. X-rays can detect the damage caused to the bone and can also detect new cells. Finally, a bone biopsy involves collecting a sample of bone tissue.

Bone cancer most frequently occurs in children or young adults aged up to 20 years and in people who have undergone radiotherapy. People who suffer from Paget's disease are susceptible to bone cancer. A predisposition to bone cancer may be hereditary. Hereditary renoblastoma can lead to bone cancer in young children. People with Li-fraumeni syndrome and children born with an umbilical hernia are susceptible to bone cancer as well.

The American Cancer Society estimates that 3,020 new cases of bones and joints cancer will be diagnosed in the year 2018 and 1,460 deaths due to bone cancer are expected. Primary bone cancer accounts for <0.2% of all cancers. In adults, over 40% of primary bone cancers are chondrosarcomas. Further, osteosarcomas accounts for 28%, chordomas 10%, Ewing tumors 8% and malignant fibrous histiocytoma/fibrosarcomas 4% of bone cancers. The remaining cases constitute several rare types of bone cancers. In children and teenagers aged <20 years, osteosarcoma accounts for 56% and Ewing tumors for 34%, being much more common than chondrosarcomas which account for 6%. Chondrosarcomas develop primarily in adults and chordomas also are most commonly found in adults with <5% of these cancers occurring in patients younger than 20 years old. Both osteosarcomas and Ewing tumors occur most frequently in children and teenagers. Siegel *et al.* (2014) estimated the number of persons who would be affected by different cancers and the overall number of cancer related deaths for the year 2017 (Table 1).

Segmentation is an approach in which pixels are grouped to form a cluster. Each pixel is assigned to the

Table 1: Estimated new cancer diagnoses and deaths from cancer in 2017

Cancer type	Estimated new diagnoses in 2017			Estimated deaths in 2017		
	Male	Female	Total	Male	Female	Total
Bones	1,680	1,340	3,020	830	630	1,460
Eye	1,440	1,290	2,730	130	180	310
Breast	2,360	232,670	235,030	430	40,000	40,430
Colon	48,450	48,380	6,830	26,270	24,040	50,310
Lung	116,000	108,210	224,210	86,930	72,330	159,260
Brain	12,820	10,560	23,380	8,090	6,230	14,320

cluster whose centroid is the nearest. Pixels having homogeneous characteristics belong to the same cluster and pixels in the same cluster must follow the homogeneity criteria of that cluster. To perform clustering and classification, k study-means, fuzzy C-mean clustering, SVM, fuzzy theory, probabilistic neural networks and learning vector quantization methods are used. However, in these methods, the segmentation of medical images is not sufficiently effective and the accuracy levels are relatively low. In cluster-based image segmentation techniques, the number of clusters must be specified a prior which reduces the atomicity of the technique. An additional major drawback in these methods is that they are sensitive to noise and therefore, the accuracy and the performance are degraded. To overcome this problem in this study, a new approach is proposed for bone cancer detection that uses mean intensity thresholding.

The fundamental method used in this study can be explained as follows. First, gray scale images of the bone are used because this leads to no loss of information. The area of bone tumor is extracted from the images using a region growing technique. The image tumor area is selected from the original image. Then the number of pixels N in the tumor area and the sum of pixel intensities S are calculated. Using N and S, the mean intensity is calculated.

Literatvre review: In this study, a method for detecting bone cancer by applying k-means clustering and mean intensity thresholding to images is introduced. Verma *et al.* (2011) introduced a single seeded region-growing technique for color image segmentation. For segmenting the color image, an intensitybased similarity index is used for the grow formula and Otsus adaptive thresholding is used to calculate stopping criteria for the grow formula. In their study, they compared the Otsus adaptive thresholding with the watershed technique. Finally, the results were compared based on Lius F-factor. Their proposed method did not require region merging steps as a post-segmentation procedure which leads to a computational time increase. Zanaty (2013) proposed a new method for automatic calculation

of the threshold for segmenting MRI images to overcome the problem of poor image contrast leading to the loss of boundary information. Here, the homogeneity criterion and probability are calculated for each pixel to achieve relatively accurate segmentation in gray matter or white matter MRI datasets.

Athanasiadis *et al.* (2006) suggested a region growing algorithm that performs on a semantic level, driven by the knowledge that each region represents at every step of the merging process. The labeling of regions leads to automatic image annotation. Semantic region growing methods are used to extract semantically meaningful objects from an image. Moorthi and Amutha (2013) proposed a method that can reasonably be implemented in Picture Archiving and Communications Systems (PACS). In their study, a segmentation process using region growing and morphological processing methods was applied because these methods are efficient and accurate. Teleradiology and digital PACS are implemented for increasing the compression ratio. Fuzzy logic is used for classification and the Region of Background (ROB) of the image is compressed using the Set Partition In the Hierarchical Tree algorithm (SPIHT). Wu *et al.* (2009) proposed a method for implementing a texture feature-based computerized method for segmenting organs in images. They used SRG algorithm for segmenting the lung parenchyma from lung CT images based on the Region Of Interest (ROI). In the preprocessing stage, each area of the lung is separated using ROIs. Then each part that appears to be a tumor/node or a cancerous area is examined closely. This method helps radiologists to diagnose the early stages of lung diseases. This method is also applicable for the liver, brain and spine diagnoses.

Bliznakova *et al.* (2014) proposed a new method and an application tool for assessing liver volume and residual function of the liver in patients with persistent kidney disease prior to the surgical intervention. In their method, liver volume segmentation, visualization and virtual cutting are performed using liver CT scan images. For CT image segmentation, a multi seeded region growing technique is used. They implemented a Software application that processes the results to produce a 3-Dimensional (3D) image of the region, allowing easy and fast validation of the segmentation results. Al-Faris *et al.* (2014) proposed an MRI breast tumor segmentation method for which they developed a customized automatic seeded region growing technique based on the Particle Swarm Optimization (PSO) image clustering system. In this method, the level set active contour and morphological thinning algorithms are used for preprocessing. Here, PSO cluster intensities are used in the automated SRG

initial seed and threshold value selection. This method shows a high performance when the results are compared with ground truths. Fan *et al.* (2005) implemented an automatic seeded region growing algorithm to provide an effectual pixel labeling technique and an automatic seed selection method for the segmentation process. Saad *et al.* (2012) presented a method for automatic segmentation of brain lesions in images obtained by diffusion-weighted magnetic resonance imaging that uses the region growing approach. A pixel intensity similarity measure and pixel mean value differences are used to detect the lesion region using region splitting and merging. A thresholding technique is applied in the automated process and comparison with the results of semi automated region growing showed that automated region growing is efficient. Kamdi and Krishna (2012) evaluated the achievements, problems encountered in the research areas of image segmentation, edge threshold, region based techniques and other segmentation techniques such as Laplacian and gradient region growing which is noise free.

In the study conducted by Kumar and Kumar (2014), an exact lung segmentation using a region growing algorithm for early detection of lung diseases and lung cancer was developed which simplified diagnosis. This method is based on the ROI: the lung area is separated from the background. Dahab *et al.* (2012) developed a probabilistic neural network model based on learning vector quantization using MRI images of the brain. In this Model, data analysis and manipulation techniques are used for the classification and detection of brain tumors. They used an edge detection algorithm and the ROI for accurately identifying the tumor area. In their study, they achieved 100% accuracy for brain tumor classification.

Sasikala and Vasanthakumar (2012) used a k-means clustering algorithm to detect cancer in a multi resolution representation of the original MRI, ultrasound and mammogram images. For segmenting the breast cancer cell they used the k-means clustering techniques. After extracting the cancer cell, they identified the stage of breast cancer using American Joint Committee on Cancer (AJCC) staging system and the Tumor Nodes Metastasis (TNM) system. To evaluate the accuracy and sensitivity of their method, they calculated the mean, standard deviation, variance and RMS values. Rajan and Prakash (2013) described a new method that uses data mining to predict lung cancer at an early stage. They developed and implemented a new data mining tool that is effective for diagnosing lung cancer in the early stages. This tool is constructed using artificial neural networks.

Rajeswari and Reena (2011) proposed a new method for classifying tumor areas. In their method, liver cancer

cell classification is performed using a support vector mechanism and fuzzy neural network classifiers. MAPSTD is applied to provide association ranking. This method is applied to liver cancer patient datasets. Doyle *et al.* (2012) introduced a Boosted Bayesian Multi Resolution (BBMR) classifier for computerized recognition of Prostate Cancer (CaP) from digitized histopathology, an obligatory precursor of automated Gleason grading. To the best of our knowledge, this research represents the first endeavor to automatically find regions involved in CaP in digital images of prostate biopsy needle cores. This approach reduces the computation time 4-6 fold as compared to non multi resolution based approaches as pixelbased classification accuracy is high.

Ganesan *et al.* (2013) proposed computer-aided diagnosis from brain cancer image segmentation and implemented a method for segmenting the brain tumor area in which the k-means algorithm used for mammograms is applied. This method improves accuracy and reduces computational time. A conventional decision tree approach is used for dataset analysis. Bandyopadhyay and Paul (2013) applied k-means clustering and DBSCAN for segmenting a tumor in MRI images of the human brain. After segmentation, they compared the results of both algorithms and concluded that the computational time increases exponentially when DBSCAN is applied.

Roy and Roy (2013) proposed an automated method for detection of brain abnormalities from MRI scan images. Tumor occupies the locations of normal tissues and their intensity values differ from normal tissues. So, it is very difficult to segment tumor from whole MRI scan image without selecting the proper threshold value based on intensity values in the image. They presented a method to find appropriate threshold intensity value which is near the intensity value of the tumor border using standard threshold value. This method allows the segmentation of tumor tissue with accuracy and location of abnormal region is also clearly identified. At the end of the process the tumor is extracted from MRI images and the shape also determined.

Leela and Kumari (2014) proposed a morphological approach for the detection of brain tumour and cancer cells. In their study, the segmentation is carried out using k-means and fuzzy c-means clustering algorithm for better performance. They compared both algorithm results and the tumor boundaries more clearly found in k-means. And tumor can be found with more precision and also fast detection is achieved in less time. After segmenting the tumour part area of the cancer part is also calculated.

Finally, concluded that k-means giving better results compared to FCM. Most of the segmentation algorithms depend on one of two basic properties that is discontinuity and similarity. The first approach partition an image based on rapid changes in intensity such as edges. The second category partitioning an image into regions based on predefined criteria. In this project second approach is used.

Kabade and Gaikwad (2013) presented a method for calculating the brain tumour shape and tumor area and its stages. Detection resists the accurate determination of stage and size of tumour. To overcome that this study uses computer aided method for segmentation of brain tumour based on the combination of two algorithms that is k-means and fuzzy C-means algorithms. This method gives the segmentation of tumour tissue with accuracy comparable to manual segmentation. In addition, it also reduces the time for computation within less time giving accurate results. At the end of the process, the tumour is extracted from the MR image after that its size, position and shape determined. The stage of the tumour is displayed based on the amount of area calculated from the segmented tumour part in brain.

Kaur and Juneja (2014) proposed a gradient differential plays an indivisible part in demarking the tumor in brain areas. Here, one benchmark set is established if that part do not match with the benchmark set are skipped by the algorithm, i.e., eminent entropy and intensity which are taken as major feature for identification of tumor in brain. If there is a benign tumor in the brain than it shows in some of the parts but if there is a malign tumor then it penetrates into deeper parts and intensity of pixels is very high in that region. These properties are very helpful to detect the tumor part in the brain and also look some of the similar features of the malign tumor in the brain.

Zade *et al.* (2012) proposed a method for early detection of breast cancer from mammograms. Mammography is the best available technique to detect cancer cell in its earlier stages. Here, seeded region growing algorithm is used for cancer region detection based on pixel intensity identification regions are separated. Here, segmentation process performed on the edge map differentiates various regions on the breast, depending on their intensity values. Each region has a different intensity value. The fatty tissues, glands, lobules and the ducts display different intensity values and thus can be separated into different regions. An abnormality such as a mass, tumors or calcifications may be present within the breast has distinctly higher intensity values than the normal tissues of the breast.

Kowar and Yadav (2012) proposed a method for brain tumor detection and segmentation using histogram thresholding. Manual segmentation of brain tumors from magnetic resonance images is a tough and time consuming task. This study presents a new technique for the detection of tumor in brain using segmentation and histogram thresholding. The proposed method can be successfully applied to detect the outline of the tumor and its geometrical dimension. The image of a brain in MRI is represented through pixel intensity. In gray color images the intensity lies between 0-255 with 0 indicating for black and 255 is assigned for the white color. The blood cells are represented by white color and 255 pixel intensity. All the gray matter is having pixel intensity <255 . First part of the present research addresses the problem of detecting the position of the tumor, i.e., whether the tumor is on the left or right side of the brain. This is achieved just with the knowledge of which part of the brain contains more numbers of the pixels having intensity around 255.

Bone cancer formation: Bone constitutes the supporting skeleton of the body. The outer part of bones consists of an arrangement of hard tissue called the matrix in which calcium salts are laid down. The hard outer layer is made of cortical bone it covers the trabecular bone inside. The outside of bone is covered with the periosteum. Some bones are hollow and the space inside them is called medullary cavity it contains soft tissue called bone marrow. The endosteum act is a tissue lining. At each end of the bone is a softer region of bone-like tissue called cartilage which is composed of a fibrous tissue matrix mixed with a gel-like substance that does not contain much calcium. Most bone is converted from cartilage. The body lays down calcium in the cartilage to form bone. After the bone formation, some cartilage may remain at the ends of the bone to act as a buffer between bones. This cartilage, together with ligaments and some other tissues form a joint between the bones. Bone itself is very rigid and strong. Bone is able to bear as much as 12,000 pounds per square inch. It takes as much as 1,200-1,800 pounds of pressure to break a thigh bone. Bone contains two types of cells. The osteoclast is the cell that is responsible for forming new bone, while the osteoclast is the cell that is responsible for softening old bone and for its resorption. The marrow of some bone is adipose tissue, while the marrow in other bones is a combination of fat and bloodforming cells. The blood-forming cells are responsible for creating red blood cells, white blood cells and blood platelets. Other cells in the marrow include plasma cells, fibroblasts and reticuloendothelial cells (Modha and Spangler, 2003).

The cause of bone cancers is not accurately known. Scientists have made great progress in discovering how certain changes in a persons DNA can cause normal cells to become cancerous. DNA may influence a person's risk of contracting certain diseases including some kinds of cancer. A gene is a unit of heredity and is a region of DNA. Genes contain the information needed to make proteins, the molecules that find out all cell functions. Some genes control the timing of cell growth and division. Genes that promote cell division are called oncogenes, while those that slow down cell division or ensure that cells die at the right time are called tumor suppressor genes. Cancer can be caused by DNA defects that initiate ontogenesis or inactivate tumor suppressor genes. Some people who suffer from cancer have DNA mutations inherited from a parent.

The American Joint Commission on Cancer staging system is used to stage all bone cancers. The factors used to determine the stage are represented by the initials T, N, M and G where T represents the description of a tumor (its size and location), N represents the spread of the cancer to lymph nodes; M represents metastasis that is the cancer's migration to distant organs and G represents the tumors grade where a higher grade indicate the presence of abnormal cells. Higher grade cancers tend to grow and spread more quickly than lower grade tumors.

MATERIALS AND METHODS

The primary purpose of the processing of bone cancer imagery proposed in this study is to identify the region of bone cancer and evaluate its mean gray scale intensity. The entire procedure is shown in Fig. 1. The method requires scan imagery of bone with or without noise. When an image containing noise such as illumination variations, occlusions, scale variations or deformation of objects is analyzed, the information retrieved may not represent the original value. Hence, the image must be denoised.

Clustering is a process in which pixels are classified based on standardized characteristics. In order to construct clusterbased segmentation, the pixels must follow the homogeneity condition of the cluster to which they are assigned. Presently, the kstudy-means (Milligan *et al.*, 1983; Guralnik and Karypis, 2001; Jarvis and Patrick, 1973; Modha and Spangler, 2003) and seeded region growing algorithm (Adams and Bischof, 1994) are most frequently used for image segmentation. K-means clustering is the method deployed in this study. It segregates the image such that the textures in a cluster have approximately the same pixel values when compared with other clusters. The k-means algorithm is an iterative

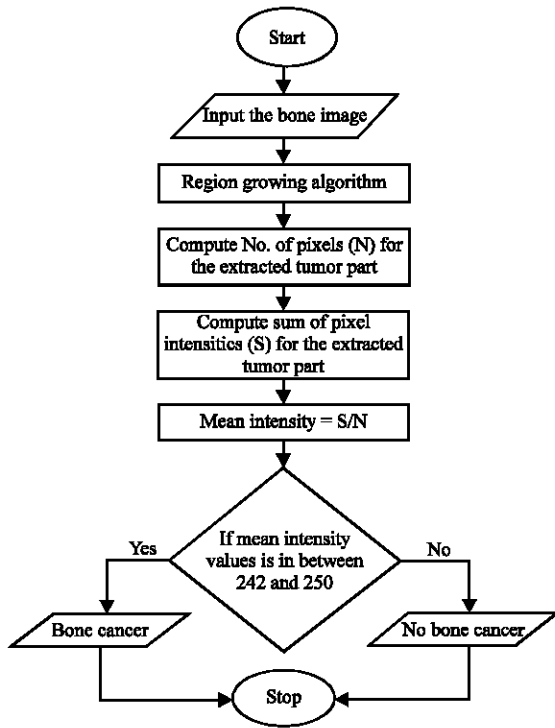


Fig. 1: Flowchart of proposed method

technique that classifies objects based on attributes, features into k number of groups. The grouping is achieved by minimizing the sum of squares of the distances between the data and the corresponding cluster centroid (Milligan *et al.*, 1983). The k -means algorithm assigns each point to the cluster whose center (centroid) is the nearest. The centre is the average of all the points in the cluster that is the arithmetic mean of its coordinates for each dimension separately over all the points in the cluster (Jarvis and Patrick, 1973). In order to predict a malignant bone tumor, a higher range k -means algorithm is adopted to cluster the points of the image into six segments using a Euclidean distance metric to avoid local minima. The major disadvantage of k -means is that it cannot build non-convex shaped clusters and that the number of clusters must be predefined. k -study-means is susceptible to noise a small number of noisy data can significantly influence the mean value. The major problem related to medical image segmentation is a required priori specification of the number of clusters. If a lower value of k is set, this may lead to better results but an increased number of iterations is required. Euclidean distance measures can unequally weight underlying factors and the computation time then increases. The steps in the k -means clustering algorithm are as follows:

- Assign a assign value for k that is number of clusters
- Randomly generate k clusters and determine the cluster centers or directly create k random points as centers of clusters
- Assign each point to the nearest cluster center
- Regenerate the new cluster centers

Currently, the seeded region growing algorithm proposed by Adams and Bischof (1994) is commonly used in the processing of medical images because it successfully segments different types of images. The algorithm does not depend on a training process. The homogeneous features of the tumors are taken into account. The first step in region growing is the selection of the required seed points. The initial region is the exact location of the seed. The regions are then grown from the seed points to adjacent points according to a region membership criterion or thresholding technique. If the principle criterion is a pixel intensity threshold value. The data are collected from the histogram of the image to establish a suitable threshold value for the region membership criterion. The four main important elements of the region growing algorithm are:

Seed point selection: The selection of seed points depends on the image. For a gray-level lighted image, segment the lightning from the background. Then observe the histogram and select the seed points from its highest range.

Collection of additional image data: The connectivity or pixel neighboring information facilitates the determination of the threshold and seed points.

Determination of thresholding value: In the region growing method, all regions must be within the threshold value which is determined prior to the process.

Checking the similarity threshold value: If the difference in the pixel-value is $<$ the similarity threshold, then the region is treated as the same region.

Several advantages of the region growing algorithm are; Region growing methods can accurately separate the regions; Region growing methods give the original images if the image has clear edges with good segmentation results. The idea is simple. Only seed point selection, that seed point grows the region. They are not sensitive to noise and therefore, their performance is high. If any noise problem occurs, it is easily overcome by using a mask to filter the holes or outliers. These are the major reasons for choosing this algorithm for segmenting bone cancer medical images.

The method described in this study facilitates the detection of cancer in a bone. In this study, the region growing method is used for extracting the tumor part. The basic steps of the algorithm are as follows:

- Select seed pixels within the image
- From each seed pixel grow a region
- Set the region prototype to be the seed pixel
- Calculate the similarity between the region prototype and the candidate pixel
- Calculate the similarity between the candidate and its nearest neighbor in the region
- Include the candidate pixel if both similarity measures are smaller than the experimentally set thresholds
- Update the region prototype by calculating the new principal component
- Go to the next pixel to be examined

In this method, the center pixel of the image is selected as the seed and the region grown according to the growing formula with a stopping criterion that determines the threshold. The flow graph for the method proposed in this study is shown in Fig. 1. First images of bone cancer are taken from the radiology assistant site. For this study, 400 bone cancer MRI images were downloaded. From these images, the tumor part is extracted using the region growing algorithm. Gray scale images are used for extracting the tumor part by using the algorithm which was developed using MATLAB Software and the threshold is set to 0.045 for extracting the cancer part accurately from the bone images. The cancer or tumor part of the image is identified and saved for further processing. Using another code, the Number of pixels (N) in the extracted tumor part is calculated which gives the cancer affected area. Then the Sum of the pixel intensities (S) is calculated. S and N are used in the calculation of the mean intensity value of the tumor part. If the mean intensity value of the tumor part is between 242 and 250, cancer is detected; Otherwise, cancer is not detected. The following steps give the entire procedure:

- Read the bone cancer image
- Apply the region growing algorithm
- Extract tumor part
- Calculate the Number of pixels (N)
- Calculate the Sum of intensities (S)
- Calculate the mean intensity: the Sum of intensities Number of pixels (S/N).
- If the range is between 242 and 250, bone is detected; else, cancer is not detected

For the analysis, MRI scan images of bone cancer were acquired from the Radiology Assistant Website

(www.radiologyassistant.nl). A total of 400 bone cancer MRI images were used in the experiments. First, the affected tumor area was extracted from the MRI scan image using the k-means algorithm. Second, the Number of pixels (N) and Sum of pixel intensities (S) for the extracted tumor area were computed. Finally, the mean pixel intensity value was computed using Eq. 1. From the experimental analysis, it was established that the mean pixel intensity values lie in between 242 and 250.

$$\text{Intensity of cancer cell} = \frac{\text{Area of interest} \times \text{Mean pixel intensity value}}{\text{Area of interest}} \quad (1)$$

RESULTS AND DISCUSSION

Bone cancer detection is one of the challenging tasks that today's researchers, doctors, academicians and so on are experiencing. It must be detected at the early stages to prevent an increase in the death rate. In many research studies, various theories have been posited which have been shown to be inaccurate because the appropriate analyses were not performed and various parameters that involve in the formation of bone cancer were not sufficiently studied. The mining of data from MRI images is an even more challenging and cumbersome task, since, it involves processing not one but hundreds of MRI images in order to extract the required results.

The bone cancer images obtained from the Radiology Assistant Website (www.radiologyassistant.nl) are used in the analyses for the identification of bone cancer. The radiologist Robin Smithuis proposed that the Radiology Assistant of the Radiology Society of the Netherlands should provide state-of-the-art radiological education for radiology residential and radiologists. The free accessibility of this information reflects the obligation of the Radiology Assistant to make knowledge affordable to a wide audience. In the experiments, around 400 images were analyzed to compute the success rate of the proposed detection method.

The segmentation process using k-means clustering and region growing was applied for the original images shown in Fig. 2a -5a to detect the area affected by cancer; and the segmented images for k-means clustering are shown in Fig. 2b -5b, respectively and Region growing in Fig. 2-5c, respectively. The entire process is implemented in MATLAB R2011a using the image processing tool box which provides image segmentation algorithms, tools and a comprehensive environment for data analysis, visualization and algorithm development.

In order to classify targeted areas as cancer or not cancer, the mean pixel intensity values are extracted for the segmented images. This image mean intensity value

Table 2: Comparison values for the images in the database

Image number	Observed result	k-means				Region growing			
		No.of pixels	Mean intensity	Experimental	Prediction	No.of pixels	Mean intensity	Experimental result	Prediction
1	Cancer	29	234.72	Not cancer	False	9	243.22	Cancer	True
2	Cancer	590	245.63	Cancer	True	217	246.84	Cancer	True
3	Cancer	121	234.57	Not cancer	False	69	244.30	Cancer	True
4	Cancer	1183	241.64	Not cancer	False	573	248.13	Cancer	True
5	Cancer	72	238.14	Not cancer	False	80	244.93	Cancer	True
6	Cancer	879	241.79	Not cancer	False	420	245.82	Cancer	True
7	Cancer	1505	248.71	Cancer	True	237	248.17	Cancer	True
8	Cancer	644	242.03	Cancer	True	284	246.03	Cancer	True
9	Cancer	455	240.58	Not cancer	False	128	244.88	Cancer	True
10	Cancer	653	242.53	Cancer	True	317	244.24	Cancer	True
11	Cancer	2655	243.16	Cancer	True	5	244.40	Cancer	True
12	Cancer	50	240.46	Not cancer	False	14	244.00	Cancer	True
13	Cancer	1084	247.37	Cancer	True	221	247.55	Cancer	True
14	Cancer	573	235.61	Not cancer	False	592	246.30	Cancer	True
15	Cancer	1313	239.03	Not cancer	False	15	244.00	Cancer	True
16	Cancer	196	240.54	Not cancer	False	86	244.66	Cancer	True
17	Cancer	26	239.54	Not cancer	False	21	244.43	Cancer	True
18	Cancer	538	244.16	Cancer	True	165	246.85	Cancer	True
19	Cancer	178	243.15	Cancer	True	336	245.81	Cancer	True
20	Cancer	1523	242.98	Cancer	True	583	247.19	Cancer	True
21	Cancer	1284	238.03	Not cancer	False	552	244.38	Cancer	True
22	Cancer	10	240.20	Not cancer	False	4	248.50	Cancer	True
23	Cancer	50	239.50	Not cancer	False	74	246.47	Cancer	True
24	Cancer	2114	248.04	Cancer	True	599	245.98	Cancer	True
25	Cancer	4905	240.80	Not cancer	False	1105	245.60	Cancer	True
26	Cancer	174	240.33	Not cancer	False	91	245.099	Cancer	True
27	Cancer	1775	242.99	Cancer	True	685	249.20	Cancer	True
28	Cancer	636	245.81	Cancer	True	273	248.11	Cancer	True
29	Cancer	1823	237.21	Not cancer	True	496	247.86	Cancer	True
30	Cancer	826	238.25	Not cancer	True	614	245.65	Cancer	True
31	Cancer	370	239.95	Not cancer	True	114	246.08	Cancer	True
32	Cancer	321	242.07	Cancer	True	177	246.17	Cancer	True
33	Cancer	305	241.92	Not cancer	False	96	244.46	Cancer	True
34	Cancer	539	246.44	Cancer	True	246	247.20	Cancer	True
35	Cancer	327	237.47	Not cancer	False	273	249.60	Cancer	True
36	Cancer	279	243.00	Cancer	True	158	248.36	Cancer	True
37	Cancer	360	242.37	Cancer	True	40	242.68	Cancer	True
38	Cancer	36	232.92	Not cancer	False	4	247.25	Cancer	True
39	Cancer	2326	247.62	Cancer	True	1039	248.61	Cancer	True
40	Cancer	1937	247.58	Cancer	False	800	248.19	Cancer	True

plays an important role in the classification. It is observed that as the tumor size increases, the mean intensity value varies. In experiment using 400 images, it was observed and established that the mean intensity values for the classification into cancer or not cancer lies between 242 and 250. The examples using region growing algorithm clearly show that, the proposed method outperforms other methods, having an average accuracy of 100% as shown in Table 2.

The preliminary results of the classification of a sample of 40 images into cancer or not cancer are shown in Table 2. As an example, let us consider image 9 in region growing algorithm. Its computed mean intensity is 244 which falls into the established range of 242-250. The predicted experimental result is cancer which is the same as the observed result. Hence, the prediction is true. Similarly, consider the same image 9 in kstudy-means, its

computed mean intensity is 240. The predicted experimental result is not cancer and the observed result is cancer. Hence, the prediction is false. By observing Table 2, it can be clearly seen that region growing algorithm gives more accurate results when compare to k-means.

The graphs plotted in Fig. 6 show the number of pixels against the number of images for the k-means and region growing algorithms in the detection of bone cancer. These data are also presented in Table 2. The number of pixels in the part affected by cancer according to both algorithms is shown in the table. A comparison of Fig. 2b and c clearly shows that the region growing algorithm yields the tumor part accurately without any noise. Therefore, the number of pixels in the tumor part or the part affected by cancer is usually smaller than when k-means is applied. This difference causes to the

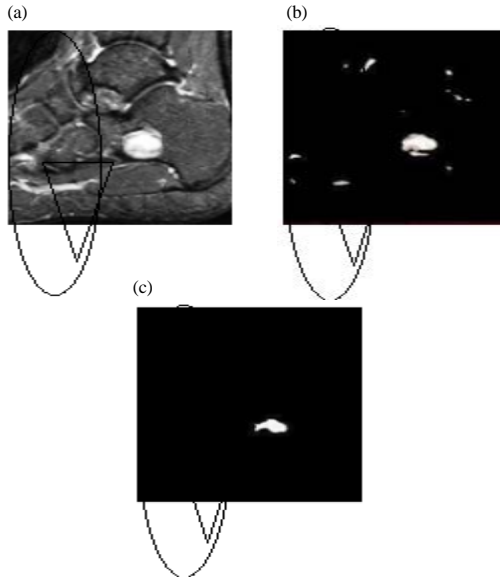


Fig. 2: Clustering applied to a navicular bone in the foot: a) MRI image of foot; b) Tumor part using k-means and c) Tumor part using region growing

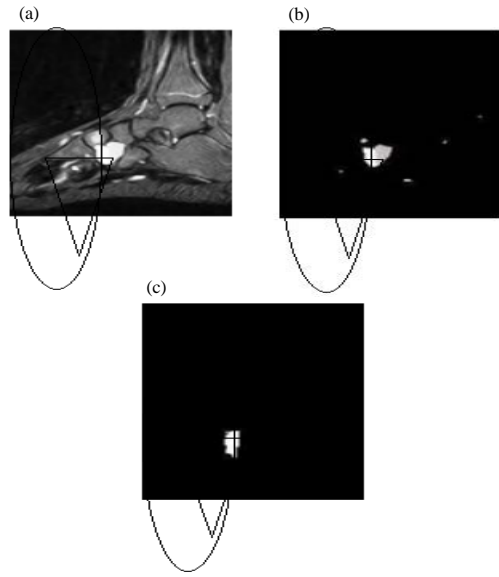


Fig. 4: Clustering applied to a Cuneiform bone in the foot: a) MRI image of foot; b) Tumor part using k-means and c) Tumor part using region growing

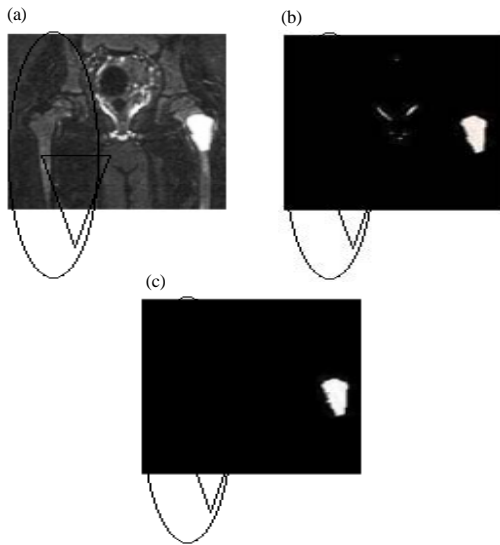


Fig. 3: Clustering applied to a femur bone in the thigh: a) MRI image of thigh; b) Tumor part using k-means and c) Tumor part using region growing

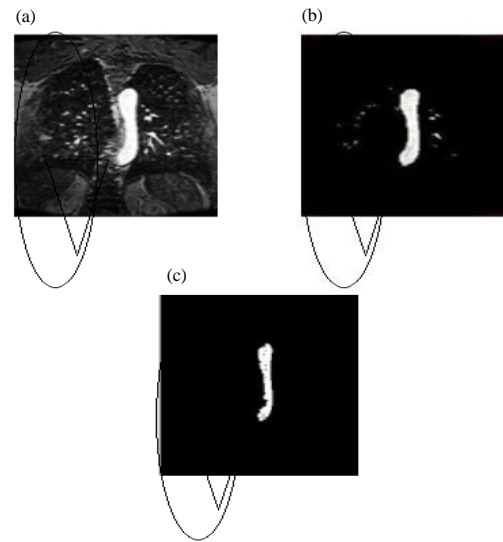


Fig. 5: Clustering applied to a sternum bone in the thorax: a) MRI image of thorax; b) Tumor part using k-means and c) Tumor part using region growing

fact that unwanted data or noise is added in k-means segmented images which leads to a greater number of pixels being located in the part affected by cancer when k-means is applied than when the region growing algorithm is applied.

Figure 7 provides a graph that shows the mean intensity values in relation to the number of images for the k-means and region growing algorithms. The mean

intensity values of both algorithms are shown in Table 2. Table 2 shows that, the region growing algorithm mean intensity values for every tumor part or part affected by cancer are higher than those of k-means. This difference is due only to the fact that unwanted data or noise is added in k-means segmented images. If the number of pixels in the cancer part increases, then the sum of the

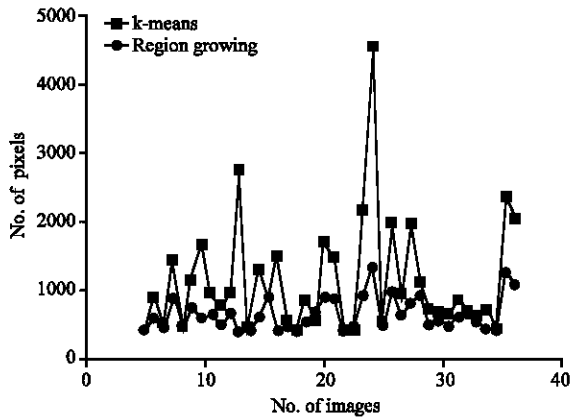


Fig. 6: Number of images vs. number of pixels

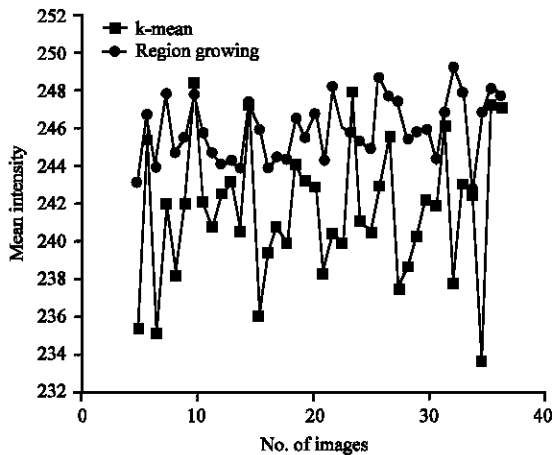


Fig. 7: Number of images vs. mean intensity

pixel intensities in the cancer part also increases which directly decreases the mean intensity values because the k-means mean intensity values are lower than those of the region growing algorithm.

Figure 8 provides a graph that shows the accuracy in relation to the number of images. It shows that the results of the method are more accurate than those of the k-mean and the region growing method. In this study, 400 images were used for testing the methods and the experimental values of both algorithms were compared, it is clear that when k-means was applied, out of 100 images, 50 yielded correct predictions and 50 yielded incorrect predictions. This means that when k-means is applied, the accuracy rate is reduced to 50%. In the present study, when the region growing algorithm was applied, 100 out of 100 images yielded correct predictions and no incorrect predictions occurred. The accuracy of the region growing algorithm is 100%. Thus, the results presented above are more accurate than those produced by the earlier methodology.

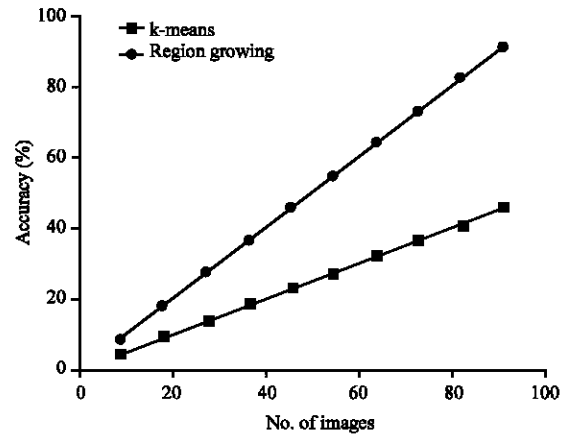


Fig. 8: Number of images vs. accuracy

CONCLUSION

This study discussed about primarily the detection of bone cancer. The proposed method can be further extended to identifying the stages of cancer. Cancer is an important factor in the global burden of disease. The estimated number of new cases worldwide each year is expected to rise from 10 million in 2002-15 million by 2025 with 60% of cases occurring in developing countries. This study presented a formal mechanism for using mean pixel intensity values to discriminate between cancer and non-cancerous areas in images. In this method, an approach for segmenting a tumor or malignant area from an image using a single seeded region growing algorithm is applied. The extracted segmented image is further processed to evaluate the mean pixel value intensity of area of interest. Based on the mean pixel intensity value thresholding, a more accurate detection of bone cancer is achieved. It was demonstrated experimentally that the resulting mechanism out-performs when compared with k-means. Thus, the discrimination between cancerous and non cancerous areas by making use of clustering using mean pixel intensity was shown to be efficient. In this study, the computer-aided diagnostic system that identifies bone cancer in CT scan images or MRI images was proposed. The method is also applicable to medical images in the original format of DICOM (Digital Imaging Communication of Medicine).

REFERENCES

Adams, R. and L. Bischof, 1994. Seeded region growing. *IEEE Trans. Pattern Anal. Mach. Intell.*, 16: 641-647.

- Al-Faris, A.Q., U.K. Ngah, N.A.M. Isa and I.L. Shuaib, 2014. Breast MRI tumour segmentation using modified automatic seeded region growing based on particle swarm optimization image clustering. Proceedings of the 17th Online World Conference on Soft Computing in Industrial Applications, November 21, 2013, Springer, Cham, Switzerland, ISBN:978-3-319-00929-2, pp: 49-60.
- Athanasiadis, T., Y. Avrithis and S. Kollias, 2006. A semantic region growing approach in image segmentation and annotation. Proceedings of the 1st International Workshop on Semantic Web Annotations for Multimedia, May 22, 2006, Edinburgh International Conference Centre, Edinburgh, Scotland, pp: 1-5.
- Bandyopadhyay, S.K. and T.U. Paul, 2013. Segmentation of brain Tumour from MRI image analysis of K-means and DBSCAN clustering. *Intl. J. Res. Eng. Sci.*, 1: 48-57.
- Bliznakova, K., N. Kolev, Z. Bliznakov, I. Buliev and A. Tonev *et al.*, 2014. Image processing tool promoting decision-making in liver surgery of patients with chronic kidney disease. *J. Software Eng. Appl.*, 7: 118-127.
- Dahab, D.A., S.S.A. Ghoniemy and G.M. Selim, 2012. Automated brain tumor detection and identification using image processing and probabilistic neural network techniques. *Int. J. Image Process. Visual Commun.*, 1: 1-8.
- Doyle, S., M. Feldman, J. Tomaszewski and A. Madabhushi, 2012. A boosted Bayesian multiresolution classifier for prostate cancer detection from digitized needle biopsies. *IEEE. Trans. Biomed. Eng.*, 59: 1205-1218.
- Fan, J., G. Zeng, M. Body and M.S. Hacid, 2005. Seeded region growing: An extensive and comparative study. *Pattern Recognit. Lett.*, 26: 1139-1156.
- Ganesan, K., U.R. Acharya, C.K. Chua, L.C. Min and K.T. Abraham *et al.*, 2013. Computer-aided breast cancer detection using mammograms: A review. *IEEE. Rev. Biomed. Eng.*, 6: 77-98.
- Guralnik, V. and G. Karypis, 2001. A scalable algorithm for clustering sequential data. Proceedings of the IEEE International Conference on Data Mining, November 29-December 2, 2001, San Jose, CA., USA., pp: 179-186.
- Jarvis, R.A. and E.A. Patrick, 1973. Clustering using a similarity measure based on shared near neighbors. *IEEE Trans. Comput and C-22*: 1025-1034.
- Kabade, R.S. and M.S. Gaikwad, 2013. Segmentation of brain tumour and its area calculation in brain MR images using K-mean clustering and fuzzy C-mean algorithm. *Int. J. Comput. Sci. Eng. Technol.*, 4: 524-531.
- Kamdi, S. and R.K. Krishna, 2012. Image segmentation and region growing algorithm. *Int. J. Comput. Technol. Electron. Eng.*, 2: 103-107.
- Kaur, N. and M. Juneja, 2014. A novel approach of brain tumor detection using hybrid filtering. *Int. J. Eng. Res. Applic.*, 4: 100-104.
- Kowar, M.K. and S. Yadav, 2012. Brain tumor detection and segmentation using histogram thresholding. *Int. J. Eng. Adv. Technol.*, 1: 16-20.
- Kumar, S. and A. Kumar, 2014. Lung segmentation using region growing algorithm. *Int. J. Adv. Res. Comput. Sci. Software Eng.*, 4: 184-187.
- Leela, G.A. and H.M.V. Kumari, 2014. Morphological approach for the detection of brain tumour and cancer cells. *J. Electron. Commun. Eng. Res.*, 2:7-12.
- Milligan, G.W., S.C. Soon and L.M. Sokol, 1983. The effect of cluster size, dimensionality and the number of clusters on recovery of true cluster structure. *IEEE Trans. Pattern Anal. Mach. Intell.*, 5: 40-47.
- Modha, D.S. and W.S. Spangler, 2003. Feature weighting in K-means clustering. *Mach. Learn*, 52: 217-237.
- Moorthi, M. and R. Amutha, 2013. High quality model for compression of medical images in telemedicine. *Scient. Res. Essays*, 8: 2022-2030.
- Rajan, J.R. and J.J. Prakash, 2013. Early diagnosis of lung cancer using a mining tool. *Intl. J. Emerging Trends Technol. Comput. Sci.*, 1: 1-4.
- Rajeswari, P. and G.S. Reena, 2011. Human liver cancer classification using microarray gene expression data. *Int. J. Comput. Applic.*, 34: 25-37.
- Roy, P. and S. Roy, 2013. An automated method for detection of brain abnormalities and tumor from MRI images. *Int. J. Adv. Res. Comput. Sci. Software Eng.*, 3: 1583-1589.
- Saad, N.M., S.A.R. Abu-Bakar, S. Muda, M. Mokji and A.R. Abdullah, 2012. Fully automated region growing segmentation of brain lesion in diffusion-weighted MRI. *IAENG Int. J. Comput. Sci.*, 39: 155-155.
- Sasikala and Vasanthakumar, 2012. Breast cancer-classification and analysis using different scanned images. *Intl. J. Image Process. Visual Commun.*, 2012: 1-7.

- Siegel, R., J. Ma, Z. Zou and A. Jemal, 2014. Cancer statistics, 2014. CA. Cancer J. Clinicians, 64: 9-29.
- Verma, O.P., M. Hanmandlu, S. Susan, M. Kulkarni and P.K. Jain, 2011. A simple single seeded region growing algorithm for color image segmentation using adaptive thresholding. Proceedings of the 2011 International Conference on Communication Systems and Network Technologies (CSNT'11), June 3-5, 2011, IEEE, Jammu, India, ISBN: 978-1-4577-0543-4, pp: 500-503.
- Wu, J., S. Poehlman, M.D. Noseworthy and M.V. Kamath, 2009. Texture feature based automated seeded region growing in abdominal MRI segmentation. J. Biomed. Sci. Eng., 2: 1-8.
- Zade, A.S., M. Wanjari and H. Chowhan, 2012. Detection of cancer cells in mammogram using seeded region growing method and genetic algorithm. J. Sci. Technol., 1: 15-20.
- Zanaty, E.A., 2013. Improved region growing method for Magnetic Resonance Images (MRIs) segmentation. Am. J. Remote Sens., 1: 53-60.